Article

Synthesis, Characterization, and Reactivity of a Uranyl β-Diketiminate Complex

Trevor W. Hayton, and Guang Wu

J. Am. Chem. Soc., **2008**, 130 (6), 2005-2014 • DOI: 10.1021/ja077538q

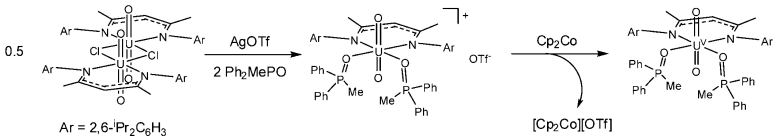

More About This Article

Additional resources and features associated with this article are available within the HTML version:

- Supporting Information
- Links to the 3 articles that cite this article, as of the time of this article download
- Access to high resolution figures
- Links to articles and content related to this article
- Copyright permission to reproduce figures and/or text from this article

View the Full Text HTML

J|A|C|S
ARTICLES
Published on Web 01/19/2008

Synthesis, Characterization, and Reactivity of a Uranyl β-Diketiminate Complex

Trevor W. Hayton* and Guang Wu

Department of Chemistry and Biochemistry, University of California Santa Barbara, Santa Barbara California 93106

Received September 30, 2007; E-mail: hayton@chem.ucsb.edu

Abstract: Addition of 1 equiv of Li(Ar_2nacnac) (Ar_2nacnac = (2,6-^{i}Pr$_2$C$_6$H$_3$)*N*C(Me)CHC(Me)*N*(2,6-^{i}Pr$_2$C$_6$H$_3$)) to an Et_2O suspension of $UO_2Cl_2(THF)_3$ generates the uranyl dimer [UO_2(Ar_2nacnac)Cl]$_2$ (**1**) in good yield. A second species can be isolated in low yield from the reaction mixtures of **1**, namely [Li(OEt_2)$_2$][UO_2(Ar_2-nacnac)Cl_2] (**2**). The structures of both **1** and **2** have been confirmed by X-ray crystallography. Complex **1** reacts with Ph_3PO to generate UO_2(Ar_2nacnac)Cl(Ph_3PO) (**3**). In addition, **1** reacts with AgOTf and either 1 equiv of $DPPMO_2$ or 2 equiv of Ph_2MePO to provide [UO_2(Ar_2nacnac)($DPPMO_2$)][OTf] (**4**) and [UO_2(Ar_2-nacnac)(Ph_2MePO)$_2$][OTf] (**5**), respectively. Both **4** and **5** have been fully characterized, including analysis by X-ray crystallography and cyclic voltammetry. Reduction of **4** with Cp_2Co provides UO_2(Ar_2nacnac)-(CH{Ph_2PO}$_2$) (**6**), a uranyl(VI) complex that is generated by the formal loss of H• from the $DPPMO_2$ ligand. Labeling studies have been performed in an attempt to elucidate the mechanism of hydrogen loss. In contrast, reduction of **5** with Cp_2Co provides UO_2(Ar_2nacnac)(Ph_2MePO)$_2$ (**7**), a rare example of a uranyl-(V) complex. As expected, the solid-state molecular structure of **7** reveals slightly longer U−O(oxo) bond lengths relative to **5**. Furthermore, complex **7** can be converted back into **5** by oxidation with AgOTf in toluene.

Introduction

The actinyl ions, AnO_2^{n+} (where An = U, Np, Pu; n = 1, 2), are ubiquitous chemical species, characterized by a linear O═An═O geometry, short An−O bonds, and substitutionally inert oxo ligands.[1] Unlike neptunyl and plutonyl, which are stable in multiple oxidation states,[2] uranium is only fleetingly stable as UO_2^+. In aqueous solutions, this species rapidly disproportionates to UO_2^{2+} and U^{4+}(aq) (eq 1).[3] However, [UO_2-(aq)]$^+$ can be stabilized at low pH (pH 2−3)[4] or in concentrated carbonate solutions,[5,6] where in each environment it exhibits a considerably longer half-life.

$$2[UO_2(aq)]^+ + 4H^+ \rightarrow [UO_2(aq)]^{2+} + U^{4+}(aq) + 2H_2O \quad (1)$$

The disproportionation of UO_2^+ has been the subject of many studies, and a recent theoretical investigation points to the intermediacy of an oxo-bridged dimer **I** (also known as a cation−cation complex) during the course of the reaction.[7]

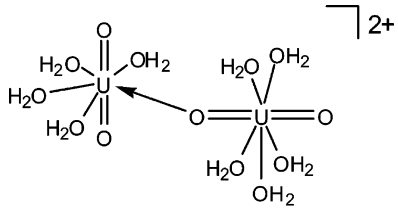

I

In anhydrous environments, UO_2^+ has been generated electrochemically and observed spectroscopically,[8−10] but it has never been isolated using this route. In contrast, a stable crystalline UO_2^+ complex can be isolated by chemical oxidation of $UI_3(THF)_4$ with pyridine-*N*-oxide[11] or by reduction of UO_2I_2-$(THF)_3$ with cyclopentadienide,[12] where, in both cases, [UO_2-$(py)_5$]$^+$ is the product isolated. Uranyl(V) can also be efficiently generated upon photolysis of uranyl(VI) in the presence of alkanes or alcohols (eq 2).[13−15] In the solid state, UO_2^+ has only been structurally characterized a few times, in crystals of

(1) Denning, R. G. *Struct. Bonding* **1992**, *79*, 215−276.
(2) Katz, J. J.; Seaborg, G. T.; Morss, L. R. *The Chemistry of the Actinide Elements*, 2nd ed.; Chapman and Hall: New York, 1986; Vol. 1.
(3) Ekstrom, A. *Inorg. Chem.* **1974**, *13*, 2237.
(4) Selbin, J.; Ortego, J. D. *Chem. Rev.* **1969**, *69*, 657−671.
(5) Docrat, T. I.; Mosselmans, J. F. W.; Charnock, J. M.; Whiteley, M. W.; Collison, D.; Livens, F. R.; Jones, C.; Edminston, M. J. *Inorg. Chem.* **1999**, *38*, 1879−1822.
(6) Ikeda, A.; Hennig, C.; Tsushima, S.; Takao, K.; Ikeda, Y.; Scheinost, A. C.; Bernhard, G. *Inorg. Chem.* **2007**, *46*, 4212−4219.
(7) Steele, H.; Taylor, R. J. *Inorg. Chem.* **2007**, *46*, 6311−6318.
(8) Kim, S.-Y.; Asakura, T.; Morita, Y.; Ikeda, Y. *J. Alloys Compd.* **2006**, *408*−*412*, 1291−1295.
(9) Mizuoka, K.; Ikeda, Y. *Radiochim. Acta* **2004**, *92*, 631−635.
(10) Shirasaki, K.; Yamamura, T.; Shiokawa, Y. *J. Alloys Compd.* **2006**, *408*−*412*, 1296−1301.
(11) Natrajan, L.; Burdet, F.; Pécaut, J.; Mazzanti, M. *J. Am. Chem. Soc.* **2006**, *128*, 7152−7153.
(12) Berthet, J.-C.; Siffredi, G.; Thuéry, P.; Ephritikhine, M. *Chem. Commun.* **2006**, 3184−3186.
(13) Howes, K. R.; Bakac, A.; Espenson, J. H. *Inorg. Chem.* **1988**, *27*, 791−794.
(14) Nagaishi, R.; Katsumura, Y.; Ishigure, K.; Aoyagi, H.; Yoshida, Z.; Kimura, T.; Kato, Y. *J. Photochem. Photobiol. A* **2002**, *146*, 157−161.
(15) Wang, W. D.; Bakac, A.; Espenson, J. H. *Inorg. Chem.* **1995**, *34*, 6034−6039.

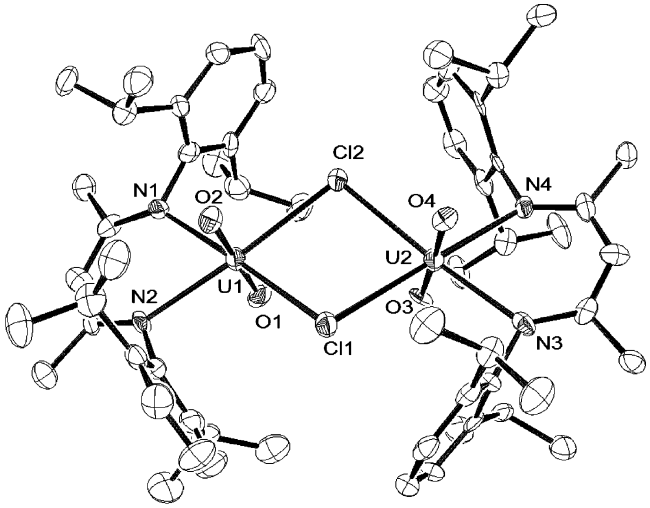

Figure 1. Solid-state molecular structure of $[UO_2(Ar_2nacnac)Cl]_2$ (**1**). Selected bond lengths (Å) and angles (deg): U1−O1 = 1.760(8), U1−O2 = 1.745(7), U2−O3 = 1.768(7), U2−O4 = 1.748(7), U1−N1 = 2.39(1), U1−N2 = 2.420(8), U2−N3 = 2.38(1), U2−N4 = 2.401(9), U1−Cl1 = 2.780(3), U1−Cl2 = 2.778(3), U2−Cl1 = 2.797(3), U2−Cl2 = 2.767(3), O1−U1−O2 = 179.4(4), O3−U2−O4 = 178.1(4), N1−U1−N2 = 71.7-(3), N3−U2−N4 = 73.3(3), Cl1−U1−Cl2 = 77.68(8), Cl1−U2−Cl2 = 77.59(8).

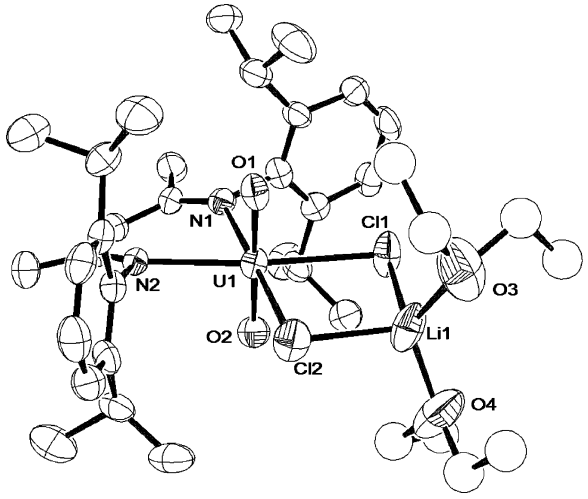

Figure 2. Solid-state molecular structure of $[Li(OEt_2)_2][UO_2(Ar_2nacnac)-Cl_2]$ (**2**). Selected bond lengths (Å) and angles (deg): U1−O1 = 1.743(6), U1−O2 = 1.753(6), U1−N1 = 2.431(7), U1−N2 = 2.414(7), U1−Cl1 = 2.727(2), U1−Cl2 = 2.743(2), Li1−Cl1 = 2.39(2), Li1−Cl2 = 2.35(2), Li1−O3 = 1.94(2), Li1−O4 = 1.95(2), O1−U1−O2 = 179.1(3), N1−U1−N2 = 72.4(2), Cl1−U1−Cl2 = 81.13(8), N1−U1−Cl1 = 100.0(2), N2−U1−Cl2 = 106.5(2).

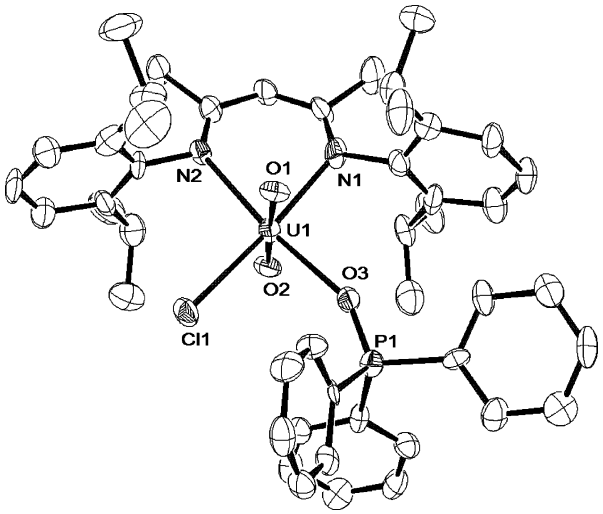

Figure 3. Solid-state molecular structure of $UO_2(Ar_2nacnac)Cl(Ph_3PO)\cdot C_6H_{14}$ (**3**·C_6H_{14}). Selected bond lengths (Å) and angles (deg): U1−O1 = 1.740(8), U1−O2 = 1.745(8), U1−O3 = 2.347(8), U1−Cl1 = 2.661(3), U1−N1 = 2.45(1), U1−N2 = 2.44(1), O1−U1−O2 = 177.6(4), N1−U1−N2 = 75.3(3), O3−U1−Cl1 = 87.1(2), N2−U1−Cl1 = 100.3(2), N1−U1−O3 = 97.4(3).

$[UO_2(py)_5][KI_2(py)_2]$,[11,12] in $[UO_2(OPPh_3)_4][OTf]$,[16] and in $\{-[UO_2(dbm)_2]_4[K_6(py)_{10}]\}^{2+}$.[17] These structural studies reveal slightly longer U−O(oxo) bonds but an overall geometry similar to that of uranyl. Uranyl(V) is also a strong reducing agent in anhydrous environments, and the U(VI)/U(V) couple has been determined to be between −1.2 and −1.7 V vs Fc/Fc^+, depending on the ligand set.[8,10,18] Similarly, in concentrated carbonate solutions, where uranyl exists as $[UO_2(CO_3)_3]^{4-}$, the U(VI)/U(V) redox potential is found at −1.1 V vs Fc/Fc^+.[5] In contrast, acidic or neutral solutions of uranyl exhibit a significantly moderated U(VI)/U(V) redox potential (approximately −0.34 V vs Fc/Fc^+).[4]

$$[UO_2(aq)]^{2+} + RH \rightarrow [UO_2(aq)]^{+} + R\bullet + H^{+} \qquad (2)$$

The strongly reducing nature of UO_2^+, along with its ability to be generated photochemically, makes uranyl an intriguing candidate in the search for a viable catalyst for solar fuel formation.[19−21] However, for the uranyl ion to be used successfully in the capture of solar energy, the properties of UO_2^+ must be better defined. In particular, for uranyl to be an effective photocatalyst the unproductive disproportionation reaction (eq 1) must be controlled.

Results and Discussion

Given the current understanding of its disproportionation reaction, we reasoned that the stabilization of UO_2^+ requires a ligand set that disfavors the formation of **I** not only by preventing dimerization along the equatorial plane but also by providing steric protection of the two uranyl oxo groups. An excellent class of coligands for this purpose are the β-diketiminates (Ar_2nacnac, Ar*N*C(Me)CHC(Me)*N*Ar). These bidentate, monoanionic ligands are easy to make, and their steric profile can be readily modified by changing the primary amine used in their initial preparation.[22,23] Most importantly, the two aryl groups would lie orthogonal to the equatorial plane of the uranyl ion, allowing the substituents on the aryl ring to provide the desired steric protection for the two uranyl oxo ligands. Given these considerations we have endeavored to ligate Ar_2nacnac (Ar = 2,6-^{i}Pr$_2$C$_6$H$_3$) to the uranyl moiety and study the redox properties of the resulting complexes.

(16) Berthet, J.-C.; Nierlich, M.; Ephritikhine, M. *Angew. Chem., Int. Ed.* **2003**, *42*, 1952−1954.
(17) Burdet, F.; Pecaut, J.; Mazzanti, M. *J. Am. Chem. Soc.* **2006**, *128*, 16512−16513.
(18) Mizuoka, K.; Tsushima, S.; Hasegawa, M.; Hoshi, T.; Ikeda, Y. *Inorg. Chem.* **2005**, *44*, 6211−6218.
(19) Jørgensen, C. K.; Reisfeld, R. *J. Electrochem. Soc.* **1983**, *130*, 681−684.
(20) Jørgensen, C. K.; Reisfeld, R. *Struct. Bonding* **1982**, *50*, 121−172.
(21) Lewis, N. S.; Nocera, D. G. *Proc. Natl. Acad. Sci. U.S.A.* **2006**, *103*, 15729−15735.
(22) Bourget-Merle, L.; Lappert, M. F.; Severn, J. R. *Chem. Rev.* **2002**, *102*, 3031−3065.
(23) Stender, M.; Wright, R. J.; Eichler, B. E.; Prust, J.; Olmstead, M. M.; Roesky, H. W.; Power, P. P. *Dalton Trans.* **2001**, 3465−3469.

Scheme 1

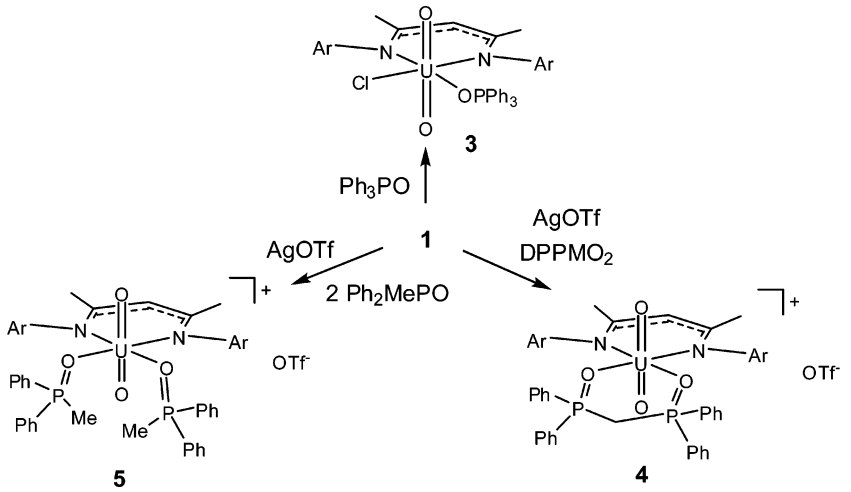

Addition of 1 equiv of Li(Ar$_2$nacnac) (Ar = 2,6-^{i}Pr$_2$C$_6$H$_3$) to a Et$_2$O suspension of $UO_2Cl_2(THF)_3$ results in a rapid color change from pale-yellow to green-brown and the formation of a white precipitate. Filtration, followed by removal of the solvent in vacuo, provides a green-brown oil. Trituration with pentane, followed by recrystallization from toluene, provides [UO_2(Ar$_2$-nacnac)Cl]$_2$ (**1**) as green-brown blocks in 81% yield (eq 3).

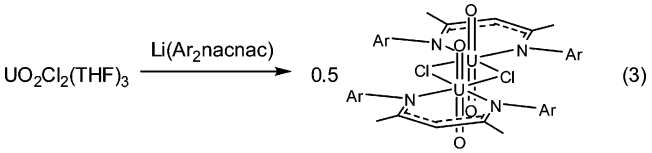

(3)

Ar = 2,6-^{i}Pr$_2$C$_6$H$_3$

1

Interestingly, no evidence for the formation of UO_2(Ar$_2$nacnac)$_2$ is ever observed, even upon addition of 2 equiv of Li(Ar$_2$nacnac) to $UO_2Cl_2(THF)_3$. Complex **1** is reasonably soluble in toluene and very soluble in CH_2Cl_2 and ethereal solvents. Its ^{1}H NMR spectrum in C_6D_6 exhibits two doublets at 0.65 and 0.89 ppm, corresponding to the two sets of diastereotopic methyl groups of the isopropyl substituents. In addition, a single septet at 3.36 ppm, corresponding to the four isopropyl methine protons, verifies the presence of a mirror plane relating both arms of the β-diketiminate ligand.

Crystals suitable for X-ray diffraction were grown from a benzene/hexanes solution. Complex **1** crystallizes in the monoclinic space group $P2_1/n$, and its solid-state molecular structure is shown in Figure 1. Complex **1** exists as a chloride-bridged dimer in the solid state. Each uranium atom in **1** exhibits octahedral coordination, while the geometry of the uranyl moiety displays metrical parameters typical of that fragment (av. U−O = 1.76 Å, av. O−U−O = 178.8°). The average U−Cl distance is 2.78 Å, while the average U−N distance is 2.39 Å. This parameter is similar to the U−N distances in the other uranium β-diketiminate complexes.[24,25] As anticipated, the aryl substituents of the β-diketiminate ligand lie orthogonal to the uranyl equatorial plane. In addition, each aryl group is tilted toward the uranium center, resulting in an average U−C(ipso) distance of 3.00 Å. The result is a bulky steric profile along the equatorial plane, effectively preventing two β-diketiminates from coordinating to one uranium center, a fact which nicely explains our synthetic results.

If solutions of complex **1** are not triturated with pentane, then the isolated product is contaminated with small amounts of a second complex, emerald green [Li(OEt$_2$)$_2$][UO_2(Ar$_2$nacnac)-Cl$_2$] (**2**), the LiCl adduct of complex **1**. Crystals of **2** were grown from solutions of Et$_2$O/hexanes, and its solid-state molecular structure is shown in Figure 2. Complex **2** exhibits a slightly distorted octahedral geometry with similar U−Cl and U−N bond lengths as complex **1** (U1−N1 = 2.431(7) Å, U1−N2 = 2.414-(7) Å, U1−Cl1 = 2.727(2) Å, U1−Cl2 = 2.743(2) Å). The metrical parameters of the uranyl moiety are also comparable to those of complex **1** and other uranyl complexes (U1−O1 = 1.743(6) Å, U1−O2 = 1.753(6) Å, O1−U1−O2 = 179.1(3)°). The lithium cation coordinates to both chloride ligands (Li1−Cl1 = 2.39(2) Å, Li1−Cl2 = 2.35(2) Å) and two molecules of diethyl ether (Li1−O3 = 1.94(2) Å, Li1−O4 = 1.95(2) Å), resulting in a tetrahedral geometry. The bond lengths and angles of the lithium cation are as expected.[26]

Complex **1** is readily derivatized and has proven to be a useful starting material. For instance, addition of 1 equiv of Ph$_3$PO to a toluene solution of **1** generates a green solution containing UO_2(Ar$_2$nacnac)Cl(Ph$_3$PO) (**3**) (Scheme 1). Complex **3** can be isolated in moderate yields by crystallization from toluene/hexanes. Its ^{1}H NMR spectrum contains two septets at 3.87 and 3.93 ppm, which correspond to the two sets of methine protons of the isopropyl substituents. These data confirm the inequivalence of the two arms of the β-diketiminate, generated upon coordination of one Ph$_3$PO. The ^{31}P{^{1}H} NMR spectrum of **3** consists of a singlet at 65.3 ppm, which is somewhat downfield when compared to other phosphine oxide complexes of uranyl.[27] Complex **3** crystallizes from toluene/hexanes as the hexane solvate, **3**·C_6H_{14}. Its solid-state molecular structure is shown in Figure 3.

Both of the metrical parameters of the two oxo ligands (U1−O1 = 1.740(8) Å, U1−O2 = 1.745(8) Å, O1−U1−O2 = 177.6-

(24) Hitchcock, P. B.; Lappert, M. F.; Liu, D. S. *J. Organomet. Chem.* **1995**, *488*, 241−248.
(25) Wright, R. J.; Power, P. P.; Scott, B. L.; Kiplinger, J. L. *Organometallics* **2004**, *23*, 4801−4803.
(26) Hitchcock, P. B.; Lappert, M. F.; Layh, M. *Dalton Trans.* **2001**, 2409−2416.
(27) Kannan, S.; Moody, M. A.; Barnes, C. L.; Duval, P. B. *Inorg. Chem.* **2006**, *45*, 9206−9212.

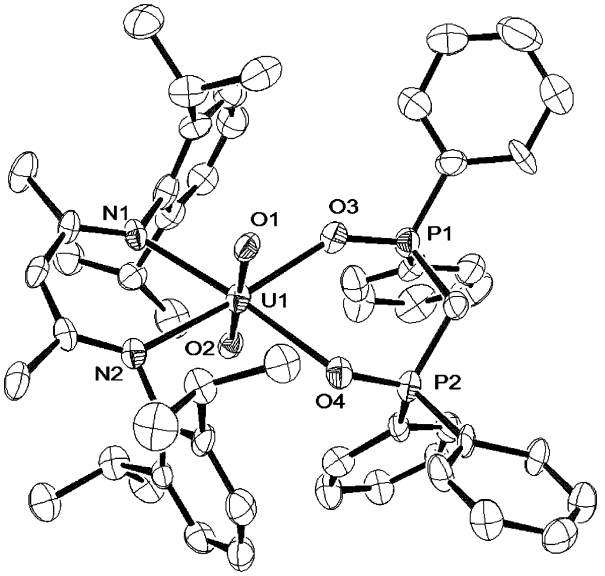

Figure 4. Solid-state molecular structure of the cation portion of $[UO_2(Ar_2\text{-nacnac})(DPPMO_2)][OTf]\cdot 2C_7H_8\cdot C_6H_{14}$ ($\mathbf{4}\cdot 2C_7H_8\cdot C_6H_{14}$). Selected bond lengths (Å) and angles (deg): U1−O1 = 1.738(6), U1−O2 = 1.736(5), U1−N1 = 2.397(7), U1−N2 = 2.397(7), U1−O3 = 2.401(6), U1−O4 = 2.405(5), O1−U1−O2 = 179.2(3), N1−U1−N2 = 70.3(2), O3−U1−O4 = 76.8(2), N1−U1−O3 = 105.9(2), N2−U1−O4 = 107.1(2).

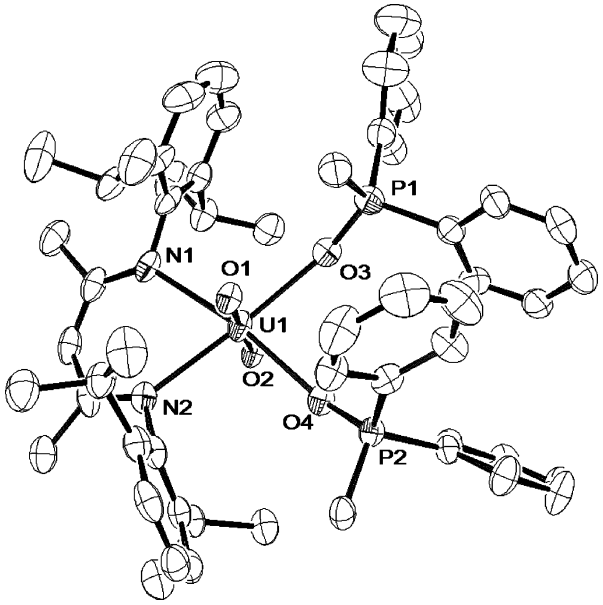

Figure 5. Solid-state molecular structure of the cation portion of $[UO_2(Ar_2\text{-nacnac})(Ph_2MePO)_2][OTf]\cdot{}^1/_2C_7H_8$ ($\mathbf{5}\cdot{}^1/_2C_7H_8$). Selected bond lengths (Å) and angles (deg): U1−O1 = 1.756(4), U1−O2 = 1.748(4), U1−O3 = 2.347(5), U1−O4 = 2.321(5), U1−N1 = 2.394(6), U1−N2 = 2.440(6), O1−U1−O2 = 177.8(2), N1−U1−N2 = 72.4(2), O3−U1−O4 = 84.3-(2), N1−U1−O3 = 104.5(2), N2−U1−O4 = 98.9(2).

(4)°) and the β-diketiminate ligand (U1−N1 = 2.45(1) Å, U1−N2 = 2.44(1) Å) are similar to those observed in **1** and **2**, while the U−O bond formed upon phosphine oxide coordination is 2.347(8) Å, comparable to that observed for $[UO_2(Ph_3PO)_4]^{2+}$.[16]

Coordination of a bidentate phosphine oxide ligand to the $UO_2(Ar_2nacnac)$ framework is also possible. For instance, addition of AgOTf to a toluene solution of **1** results in a color change to deep red. Subsequent addition of $DPPMO_2$ ($DPPMO_2$ = $Ph_2P(O)CH_2P(O)Ph_2$) generates a green-brown solution containing $[UO_2(Ar_2nacnac)(DPPMO_2)][OTf]$ (**4**) (Scheme 1), which can be isolated as green-brown blocks in good yield.

Complex **4** is somewhat soluble in arene solvents and quite soluble in THF and CH_2Cl_2. Its ^1H NMR spectrum is consistent with the presence of the β-diketiminate ligand, while the incorporation of $DPPMO_2$ is confirmed by the appearance of a triplet at 4.54 ppm (J_{PH} = 12.8 Hz), assignable to the methylene protons of the $DPPMO_2$ backbone. Furthermore, the $^{31}P\{^1H\}$ NMR spectrum of **4** consists of a single peak at 63.2 ppm, while the $^{19}F\{^1H\}$ NMR spectrum of **4** also consists of a single peak at −15.1 ppm. The IR spectrum of **4** as a KBr pellet exhibits a strong peak at 917 cm^{-1}, which we have assigned to the U=O asymmetric stretch. This is in the range of many other uranyl complexes, including $UO_2I_2(THF)_3$ (928 cm^{-1}) and $UO_2(OTf)_2(py)_3$ (943 cm^{-1}).[28,29]

Complex **4** crystallizes in the orthorhombic space group *Pbcn* as a toluene and hexane solvate, $\mathbf{4}\cdot 2C_7H_8\cdot C_6H_{14}$. Its solid-state molecular structure is shown in Figure 4. Complex **4** exhibits octahedral geometry with an η^2-$DPPMO_2$ ligand and a noncoordinating triflate anion. It exhibits similar metrical parameters for its uranyl oxo ligands (U1−O1 = 1.738(6) Å, U1−O2 = 1.736(5) Å, O1−U1−O2 = 179.2(3)°) as those observed for complex **3**. In addition, the U−N distances of the β-diketiminate ligand (U1−N1 = 2.397(7) Å, U1−N2 = 2.397(7) Å) are also comparable to those of **3**, while the U−O(phosphine oxide) distances are similar to those observed in $[UO_2(Ph_3PO)_4]^{2+}$.[16,30]

The reaction of complex **1** with AgOTf, followed by addition of 2 equiv of Ph_3PO, does not generate $[UO_2(Ar_2nacnac)(Ph_3PO)_2][OTf]$, as hoped. Instead, the product formed appears to be $UO_2(Ar_2nacnac)(Ph_3PO)(OTf)$, based on the intensities and pattern of peaks in the ^1H NMR spectrum of the crude reaction mixture. However, substitution of Ph_3PO with a less bulky analogue, namely Ph_2MePO, provides the desired product, $[UO_2(Ar_2nacnac)(Ph_2MePO)_2][OTf]$ (**5**), in reasonable yield as dark green-brown needles (Scheme 1). Complex **5** is only slightly soluble in arene solvents but quite soluble in THF and CH_2Cl_2. It exhibits a single peak in its $^{31}P\{^1H\}$ NMR spectrum at 73.6 ppm, while the methyl resonance of the phosphine oxide ligands appears as a doublet at 1.35 ppm (J_{PH} = 13.2 Hz) in its ^1H NMR spectrum. Its $^{19}F\{^1H\}$ NMR spectrum consists of a singlet at −13.6 ppm.

Complex **5** crystallizes in the triclinic space group $P\bar{1}$ as a toluene solvate, $\mathbf{5}\cdot{}^1/_2C_7H_8$. Like complex **4**, it exhibits an octahedral geometry and an uncoordinated triflate ligand (Figure 5). It also exhibits similar uranium−ligand bond distances. For instance, its U−N (U1−N1 = 2.394(6) Å, U1−N2 = 2.440(6) Å) and U−O(phosphine oxide) (U1−O3 = 2.347(5) Å, U1−O4 = 2.321(5) Å) bond lengths are similar to those of **4**, while the parameters of the uranyl moiety are normal (U1−O1 = 1.756(4) Å, U1−O2 = 1.748(4) Å, O1−U1−O2 = 177.8(2)°).

In contrast to the majority of uranyl complexes, which are bright yellow in color, the uranyl β-diketiminate complexes are an intense green-brown. For complex **1** this difference is attributable to the absorption bands at 495 nm (ϵ = 1611 $L\cdot mol^{-1}\cdot cm^{-1}$) and 657 nm ($\epsilon$ = 993 $L\cdot mol^{-1}\cdot cm^{-1}$) (Figure 6). Complex **1** also exhibits an absorption band at 403 nm (ϵ =

(28) Berthet, J.-C.; Nierlich, M.; Ephritikhine, M. *Dalton Trans.* **2004**, 2814−2821.
(29) Berthet, J.-C.; Nierlich, M.; Ephritikhine, M. *Chem. Commun.* **2004**, 870−871.
(30) Arnáiz, F. J.; Miranda, M. J.; Aguado, R.; Mahía, J.; Maestro, M. A. *Polyhedron* **2002**, *21*, 2755−2760.

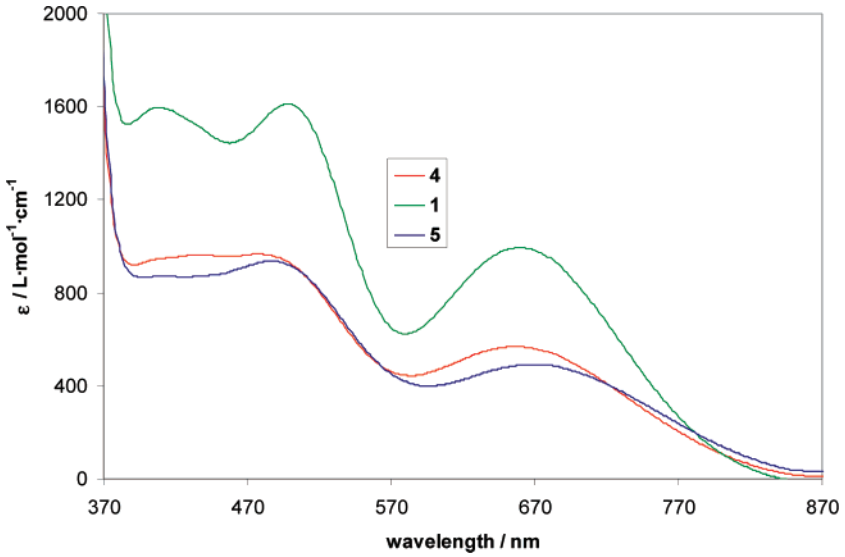

Figure 6. Room temperature absorption spectra of **1** (0.50 mM, toluene), **4** (0.96 mM, CH_2Cl_2), and **5** (0.62 mM, CH_2Cl_2).

1596 $L \cdot mol^{-1} \cdot cm^{-1}$) which may be due to the $UO_2(aq)^{2+}$ chromophore absorption (typically seen at 415 nm).[31] The absorption spectra for complexes **4** and **5** are similar (Figure 6), while the room-temperature emission spectra of **4** reveals a peak centered at 368 nm ($\lambda_{ex} = 300$ nm). Interestingly, excitation at 415 nm does not result in any observed emission, and the emission peak normally associated with uranyl (usually found at 500 to 515 nm) is never observed.[31] Duval and co-workers have observed similar results, which they attribute to a ligand-based photochemical pathway that circumvents the usual uranyl excited state.[32]

The solution redox properties of **4** and **5** have been investigated by cyclic voltammmetry. The cyclic voltammogram of complex **4** reveals an irreversible reduction wave at −1.14 V (vs Fc/Fc^+) at a scan rate of 10 mV/s (in MeCN) which we attribute to the UO_2^{2+}/UO_2^+ redox couple. Interestingly, this feature approaches reversibility as the scan rate increases (Figure 7). In contrast, the cyclic voltammogram of the same feature for complex **5** (in CH_2Cl_2) is irreversible at all scan rates. Its potential is −1.45 V at a scan rate of 200 mV/s (vs Fc/Fc^+) (see Supporting Information). The difference in reduction potential between these two species is remarkable, given their chemical similarity. Both complexes **4** and **5** exhibit irreversible oxidation features at 0.63 and 0.64 V, respectively (vs Fc/Fc^+), at a scan rate of 200 mV/s, which we attribute to oxidation of the Ar_2nacnac ligand.

The observed UO_2^{2+}/UO_2^+ redox potentials for **4** and **5** are in-line with previously reported findings. For instance, the uranyl Schiff base complex UO_2(saloph)(dmso) (saloph = *N*,*N*′-disalicylidene-*o*-phenylenediaminate) exhibits a U(VI)/U(V) couple at −1.55 V (vs Fc/Fc^+),[33] while $UO_2(dbm)_2(dmf)$ (dbm = dibenzoylmethanate) exhibits a U(VI)/U(V) couple at −1.46 V (vs Fc/Fc^+).[8]

We have attempted the chemical reduction of both complexes **4** and **5** in an attempt to understand the reactivity they undergo upon electron transfer. Thus addition of 1 equiv of cobaltocene to **4** in toluene results in the precipitation of $[Cp_2Co][OTf]$ and

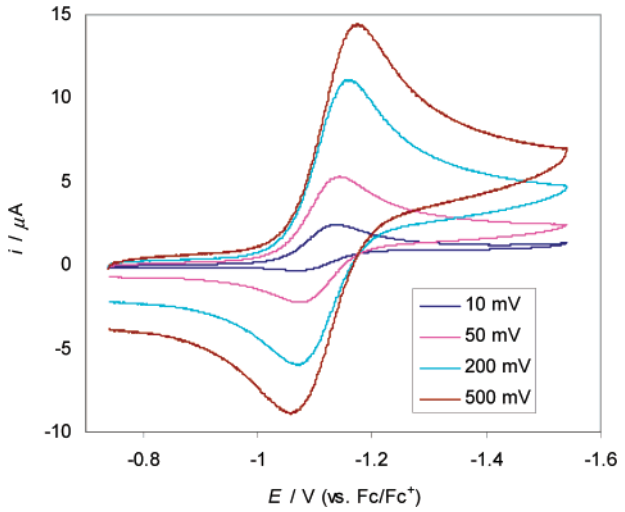

Figure 7. Room temperature cyclic voltammogram for **4** in MeCN (0.1 M $[NBu_4][PF_6]$ as supporting electrolyte).

provides a new uranium-containing species in modest yield, which we have identified as $UO_2(Ar_2nacnac)(CH\{Ph_2PO\}_2)$ (**6**) (eq 4). Complex **6** is a uranyl(VI) species that results from the

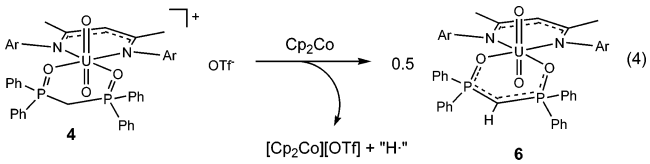

formal loss of H• from the $DPPMO_2$ ligand. The ^1H NMR spectrum of **6** is consistent with the presence of the β-diketiminate ligand in an environment where both aryl substituents are magnetically equivalent. However, the triplet at 4.54 ppm normally associated with the methylene bridge of $DPPMO_2$ is not observed; instead a broad singlet at 2.37 ppm, which integrates for only one proton, is found. This peak sharpens considerably in the $^1H\{^{31}P\}$ NMR spectrum of **6**. Consistent with the proposed formulation, the $^{31}P\{^1H\}$ NMR spectrum of **6** reveals a single peak at 64.1 ppm, while the $^{19}F\{^1H\}$ NMR spectrum is devoid of any resonances. The β-diphosphine oxide anion ligand has precedent in the chemical literature. For

(31) Baird, C. P.; Kemp, T. J. *Prog. React. Kinet.* **1997**, *22*, 87−139.
(32) Vaughn, A. E.; Bassil, D. B.; Barnes, C. L.; Tucker, S. A.; Duval, P. B. *J. Am. Chem. Soc.* **2006**, *128*, 10656−10657.
(33) Mizuoka, K.; Ikeda, Y. *Inorg. Chem.* **2003**, *42*, 3396−3398.

instance, it is formed by deprotonation of $DPPMO_2$ by either *n*-BuLi or $AlMe_3$.[34,35] Furthermore, the nitrogen analogue of the β-diphosphine oxide anion, $[CH(Ph_2P{=}NSiMe_3)]^-$, has been ligated to uranyl.[36] This ligand coordinates to the uranyl fragment in a tridentate fashion, through both nitrogen donors and the bridging methine carbon. Unfortunately, we have been unable to grow single crystals of complex **6**, and we cannot confirm the binding mode of the β-diphosphine oxide anion, which may also coordinate to uranyl through its methine carbon.

In an attempt to understand the fate of the lost hydrogen atom we have monitored this reaction by NMR spectroscopy. Upon addition of 1 equiv of Cp_2Co to a C_6D_6 solution of **4** a color change from green-brown to red is observed, and a yellow precipitate is formed. The ^1H NMR spectrum of this solution exhibits two septets at 2.98 and 3.87 ppm, in a 1:1 ratio, attributable to the methine protons of the isopropyl substituents of the Ar_2nacnac ligand, indicating the presence of two different Ar_2nacnac environments. The latter signal, along with the anticipated singlet at 2.37 ppm, is assignable to complex **6**. In addition, a new singlet is observed at 3.29 ppm, which integrates for *two* protons. We have assigned this peak to the methylene group of the β-diimine tautomer of the β-diketiminate ligand (eq 5),[37] which appears to be formed by hydrogen addition to the γ carbon of the Ar_2nacnac ligand. This molecule was selectively extracted from the reaction mixture with pentane, and its identity was confirmed by EI mass spectrometry.

To establish that the source of the extra hydrogen on the β-diimine is the hydrogen lost from the $DPPMO_2$ ligand upon reduction of **4**, we have synthesized $[UO_2(Ar_2nacnac)(DPPMO_2\text{-}d_2)][OTf]$ (**4**-d_2), which has been selectively deuterated at the methylene position of $DPPMO_2$. The ^1H NMR spectrum of a mixture of **4**-d_2 and 1 equiv of Cp_2Co in C_6D_6 also exhibits two septets at 3.87 and 2.98 ppm, in a 1:1 ratio. However, the singlet at 2.38 ppm, while present, exhibits a very small intensity, and the peak at 3.30 ppm, assigned to the methylene bridge of the β-diimine, is roughly half the relative intensity of the same peak in the nondeuterated reaction mixture. In addition, the ^2H NMR spectrum of this sample in C_6H_6 exhibits two broad singlets at 3.26 and 2.39 ppm of approximately equal intensity. This unmistakably demonstrates that the hydrogen atom lost by $DPPMO_2$ upon reduction of **4** is incorporated into a molecule of Ar_2nacnac, generating the β-diimine. It is likely that, upon reduction of **4**, $U^VO_2(Ar_2nacnac)(DPPMO_2)$ is transiently formed but quickly undergoes hydrogen loss to form complex **6** and a molecule of the β-diimine (eq 5). Several questions

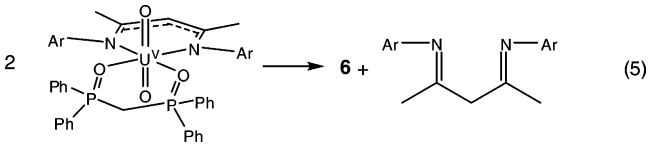

(5)

remain, however. For instance, the appearance of a small peak at 2.38 ppm indicates that some hydrogen exchange with the $DPPMO_2$ methylene bridge is somehow occurring, but the mechanism of this exchange is unclear. Furthermore, the fate of the other 0.5 equiv of uranium and the other 0.5 equiv of $DPPMO_2$ remains unknown, but it is possible that these components precipitate out with the $[Cp_2Co][OTf]$ or are NMR silent.[38]

Not surprisingly, complex **6** can also be generated by addition of a strong base, such as $NaN(SiMe_3)_2$ or KH, to a solution of **4** (eq 6). In the case of these two reagents, the only observed product in the reaction mixture is **6**, and there is no evidence for the formation of the β-diimine tautomer of the β-diketiminate ligand.

$$\mathbf{4} + \mathrm{NaN\{SiMe_3\}_2} \rightarrow \mathbf{6} + \mathrm{NaOTf} + \mathrm{HN\{SiMe_3\}_2} \quad (6)$$

We have also investigated the chemical reduction of complex **5** on a preparative scale. For instance, the reaction of complex **5** with cobaltocene in toluene generates $UO_2(Ar_2nacnac)(Ph_2MePO)_2$ (**7**) along with $[Cp_2Co][OTf]$ (eq 7). Complex **7** can

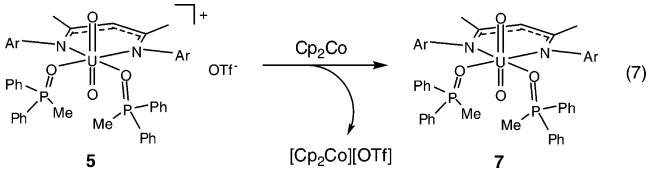

(7)

be isolated in good yield as an orange powder. The ^1H NMR spectrum of **7** is consistent with a paramagnetic uranyl(V) ion; the two signals for the diastereotopic methyl groups of the isopropyl substituents are attributed to the broad singlets at -0.31 and 11.28 ppm, while the signal for the methyl groups bound to the phosphorus atom is attributed to the broad singlet at -2.47. In addition, the $^{31}P\{^1H\}$ NMR spectrum of **7** reveals a single broad peak at -28.7 ppm (fwhm = 80 Hz), while the $^{19}F\{^1H\}$ NMR spectrum is devoid of any resonances.

Complex **7** crystallizes from a 1:1 solution of toluene and hexanes in the triclinic space group $P\bar{1}$ as a toluene solvate, $\mathbf{7}\cdot{}^1/_2C_7H_8$, and its solid-state molecular structure is shown in Figure 8. Like complex **5**, **7** possesses a distorted octahedral geometry. The U−O(oxo) bond lengths (U1−O1 = 1.810(4) Å, U1−O2 = 1.828(4) Å) are slightly longer than those of **5**; however the two oxo ligands are still in a *trans* disposition (O1−U1−O2 = 178.4(2)°). In addition, the U−N (U1−N1 = 2.530(5) Å, U1−N2 = 2.524(5) Å) and U−O(phosphine oxide) (U1−O3 = 2.457(4) Å, U1−O4 = 2.462(4) Å) bond lengths are slightly elongated, as compared to those observed in **5**. These results are completely consistent with the previously determined structures of uranyl(V).[39] For instance, the uranyl moiety in the solid-state structure of $[UO_2(Ph_3PO)_4]^+$ exhibits U−O distances of 1.821(6) and 1.817(6) Å, nearly identical metrical parameters to those observed for **7**.[16] The U−O bond lengths of **7** also closely match those reported for $[UO_2(py)_5]^+$ (U−O = 1.836(2) Å and 1.834(2) Å);[11] however in this example a dative interaction with a potassium cation may help to lengthen the U−O bond. Similarly, the calculated U−O(oxo) bond length for $[UO_2(H_2O)_5]^+$ was determined to be 1.810 Å, about 0.04 Å longer than that of the uranyl(VI) congener.[39,40]

(34) Nassar, R.; Noll, B. C.; Henderson, K. W. *Acta Crystallogr., Sect. E* **2004**, *60*, m1023−m1024.
(35) Nassar, R.; Noll, B. C.; Henderson, K. W. *Polyhedron* **2004**, *23*, 2499−2506.
(36) Sarsfield, M. J.; Steele, H.; Helliwell, M.; Teat, S. J. *Dalton Trans.* **2003**, 3443−3449.
(37) Feldman, J.; McLain, S. J.; Parthasarathy, A.; Marshall, W. J.; Calabrese, J. C.; Arthur, S. D. *Organometallics* **1997**, *16*, 1514−1516.
(38) We have also screened the reactivity of $DPPMO_2$ with Cp_2Co, with and without H(nacnac) present, and have observed no reactivity.
(39) Denning, R. G. *J. Phys. Chem. A* **2007**, *111*, 4125−4143.
(40) Hay, P. J.; Martin, R. L.; Schreckenbach, G. *J. Phys. Chem. A* **2000**, *104*, 6259−6270.

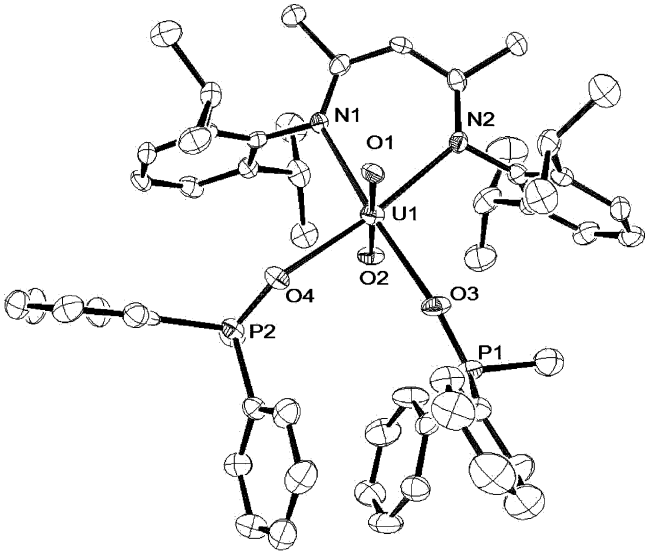

Figure 8. Solid-state molecular structure of $UO_2(Ar_2nacnac)(Ph_2MePO)_2 \cdot {}^1/_2C_7H_8$ (**7**·$^1/_2C_7H_8$). Selected bond lengths (Å) and angles (deg): U1−O1 = 1.810(4), U1−O2 = 1.828(4), U1−N1 = 2.530(5), U1−N2 = 2.524(5), U1−O3 = 2.457(4), U1−O4 = 2.462(4), O1−U1−O2 = 178.4(2), N1−U1−N2 = 72.9(2), O3−U1−O4 = 84.5(2), N1−U1−O4 = 100.7(2), N2−U1−O3 = 102.0(2).

The room-temperature absorption spectrum of complex **7** is quite different from that observed for **5** (Figure 9). In particular, the absorption at 671 nm in the UV/vis spectrum of **5** is missing in the UV/vis spectrum of **7**, which accounts for the striking color change between the two species. However, a new band is observed at 755 nm ($\epsilon = 56$ L·mol^{-1}·cm^{-1}), which is consistent with an f → f transition that is anticipated for a $5f^1$ electronic structure. Interestingly, a similar spectrum has been observed for UO_2^+ in perchloric acid.[41] We also observe a significant difference between the IR spectra of **5** and **7**. In the IR spectrum of complex **5** the asymmetric stretch of the uranyl group is assigned to the peak at 918 cm^{-1}. Upon formation of **7**, this peak disappears and a strong band at 800 cm^{-1} is observed. This value is consistent with the previously reported ν_{asy}(U═O) for UO_2^+. For instance, $[UO_2(py)_5]^+$ exhibits a ν_{asy}(U═O) of 797 cm^{-1},[11] while $UO_2(OTf)(THF)_x$ exhibits a ν_{asy}(U═O) of 853 cm^{-1}.[12] Moreover, a shift of similar magnitude is observed for $[UO_2(saloph)(DMSO)]^{0/-}$, which exhibits ν_{asy}(U═O) values of 895 and 770 cm^{-1} for the uranyl(VI) and uranyl(V) derivatives, respectively.[33]

Complex **7** has proven to be quite reactive. As expected, complex **5** is cleanly regenerated upon oxidation of **7** with AgOTf, as assayed by ^{1}H and ^{31}P{^{1}H} NMR spectroscopy. In addition, **7** reacts quickly with $DPPMO_2$ to provide complex **6** and the β-diimine tautomer of the β-diketiminate ligand, according to ^{1}H and ^{31}P{^{1}H} NMR spectroscopy (eq 8). Presumably, the reaction proceeds by substitution of the two Ph_2MePO ligands with $DPPMO_2$, and the outcome provides strong evidence in favor of the intermediacy of a U(V) complex during the formation of **6** from complex **4**.

When stored at −25 °C as a crystalline solid **7** appears to be indefinitely stable, but in the solution phase **7** exhibits a finite lifetime. For instance, solutions of **7** in C_6D_6 exhibit partial decomposition after 24 h, with complete decomposition occurring over the course of a week. The only identifiable signals after 7 days are those of H(Ar_2nacnac), identified by the characteristic chemical shift of the amine proton at 12.48 ppm in the ^{1}H NMR spectrum,[23] and uncoordinated Ph_2MePO, identified as a sharp singlet at 42.1 ppm in the ^{31}P{^{1}H} NMR spectrum. Solutions of **7** in THF-d_8 degrade much faster, with complete decomposition occurring after 20 h. Again, the only identifiable peaks in these solutions are those of H(Ar_2nacnac) and Ph_2MePO. Interestingly, both the ^{1}H and ^{31}P{^{1}H} NMR spectra of freshly prepared solutions of **7** in THF-d_8 are consistent with the presence of uncoordinated Ph_2MePO, while the signals for the Ar_2nacnac ligand are shifted from those observed in C_6D_6. This may indicate the formation of a THF complex, such as $UO_2(Ar_2nacnac)(Ph_2MePO)(THF)$. The formation of this species may explain the decreased stability of **7** in this solvent, as its coordination sphere would be less capable of protecting the uranyl(V) center. However, attempted isolation of the new complex only results in the recovery of **7**. Finally, solutions of **7** in equimolar solutions of C_6D_6/CD_2Cl_2 completely decompose over the course of 2 h, also generating H(Ar_2nacnac) and Ph_2MePO as the only identifiable products, a fact which probably explains the irreversibility of the UO_2^{2+}/UO_2^+ couple observed in the cyclic voltammogram of complex **5** in CH_2Cl_2. Unfortunately, we have not yet been able to determine the fate of the uranium in these solutions.

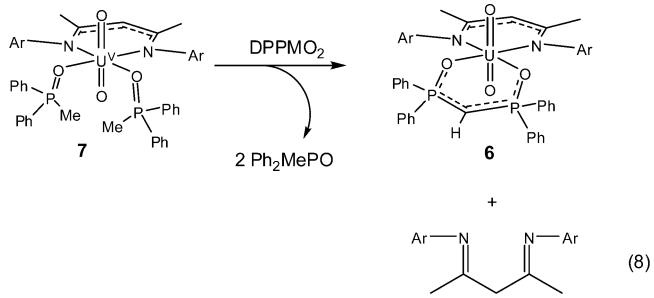

Summary

The isolation of complex **7** demonstrates that uranyl(V) can be sufficiently stabilized by using a ligand set which provides steric bulk in the uranyl equatorial plane *and* along the O═U═O axis. The Ar_2nacnac ligand set most likely blocks the formation of the "cation−cation" complex, thereby slowing the disproportionation reaction. Furthermore, the facile loss of a hydrogen atom from the $DPPMO_2$ ligand in complex **4** upon reduction indicates how important ligand choice is for stabilizing UO_2^+, as even the seemingly robust $DPPMO_2$ ligand can undergo decomposition. Removal of the methylene bridge in $DPPMO_2$ by switching to two Ph_2MePO ligands, probably the closest steric match to $DPPMO_2$, removes the acidic hydrogen and results in a ligand platform capable of stabilizing uranyl(V). While complex **7** is stable enough to be isolable as a crystalline solid, it is still quite reactive. Future studies will focus on modifying our ligand set to generate even more robust uranyl(V) derivatives. We will also continue to study the reaction chemistry of complex **7**, in particular the reactivity of the weakened uranium−oxo interactions.

Experimental Section

General. All reactions and subsequent manipulations were performed under anaerobic and anhydrous conditions under either high vacuum or an atmosphere of nitrogen or argon. THF, hexanes, diethyl ether,

(41) Bell, J. T.; Friedman, H. A.; Billings, M. R. *J. Inorg. Nucl. Chem.* **1974**, *36*, 2563−2567.

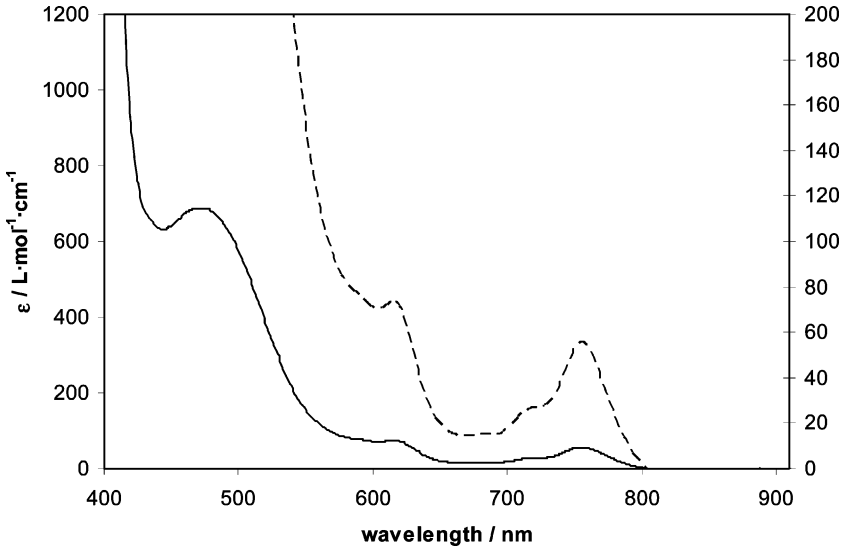

Figure 9. Room temperature absorption spectra of **7** (2.9 mM, toluene). Dashed line shows an expansion of the *y*-axis.

and toluene were dried by passage over activated molecular sieves using a Vacuum Atmospheres solvent purification system. C_6D_6, CD_2Cl_2, and THF-d_8 were dried over activated 4 Å molecular sieves for 24 h before use. $UO_2Cl_2(THF)_3$,[42] Li(Ar$_2$nacnac),[23] and $DPPMO_2$[43] were synthesized according to published procedures. All other reagents were purchased from commercial suppliers and used as received.

NMR spectra were recorded on either a Varian INOVA 400 or a Varian INOVA 500 spectrometer. ^{1}H and ^{13}C{^{1}H} NMR spectra are referenced to external $SiMe_4$ using the residual protio solvent peaks as internal standards (^{1}H NMR experiments) or the characteristic resonances of the solvent nuclei (^{13}C NMR experiments). ^{31}P{^{1}H} NMR spectra were referenced to external 85% H_3PO_4, while ^{19}F{^{1}H} NMR spectra were referenced to external α,α,α-trifluorotoluene. Elemental analyses were performed by Desert Analytics of Tuscon, AZ. UV−vis spectra were recorded on a JASCO V-570 UV−vis−NIR spectrometer, fluorescence spectra were recorded on a PTI QuantaMaster fluorimeter, and IR spectra were recorded on a Mattson Genesis FTIR spectrometer.

Cyclic Voltammetry Measurements. CV experiments were performed using a CH Instruments 600c Potentiostat, and the data were processed using CHI software (version 6.29). All experiments were performed in a glovebox using a 20 mL glass vial as the cell. The working electrode consisted of a platinum disk embedded in glass (2 mm diameter), the counter electrode was a platinum wire, and the reference electrode consisted of AgCl plated on Ag wire. Solutions employed during CV studies were typically 3 mM in the uranium complex and 0.1 M in $[Bu_4N][PF_6]$. All potentials are reported versus the $[Cp_2Fe]^{0/+}$ couple. For all trials $i_{p,a}/i_{p,c} = 1$ for the $[Cp_2Fe]^{0/+}$ couple, while $i_{p,c}$ increased linearly with the square root of the scan rate (i.e., $\sqrt{v}$). Redox couples which exhibited behavior similar to that of the $[Cp_2Fe]^{0/+}$ couple were thus considered reversible.

Synthesis of [UO$_2$(Ar$_2$nacnac)Cl]$_2$ (1). To a stirring Et_2O suspension (5 mL) containing $UO_2Cl_2(THF)_3$ (0.392 g, 0.71 mmol) was added Li(Ar$_2$nacnac) (0.298 g, 0.71 mmol). This resulted in the immediate formation of a deep green-brown solution. After stirring for 2 h, this solution was filtered through a Celite column supported on glass wool (0.5 cm × 2 cm), and the volatiles were removed in vacuo. The resulting green oil was triturated with pentane to provide a brown powder which was subsequently dissolved in toluene and filtered through a Celite column supported on glass wool. This solution was stored at −25 °C for 12 h, resulting in the precipitation of green-brown blocks (0.414 g, 0.29 mmol). 81% yield. Anal. Calcd for $C_{29}H_{41}UClN_2O_2$: C, 48.17; H, 5.71; N, 3.87. Found: C, 48.69; H, 5.67; N, 3.22. ^{1}H NMR (C_6D_6, 25 °C, 400 MHz): δ 0.65 (d, 24H, J_{HH} = 6.8 Hz, CH*Me*$_2$), 0.89 (d, 24H, J_{HH} = 6.8 Hz, CH*Me*$_2$), 1.08 (s, 12H, Me), 3.36 (septet, 8H, J_{HH} = 6.4 Hz, C*H*Me$_2$), 4.59 (s, 2H), 6.94 (br s, 4H, para CH), 7.15 (br s, 8H, meta CH, coincident with solvent resonance). ^{13}C{^{1}H} NMR (C_6D_6, 25 °C, 125 MHz) δ 24.2 (Me), 27.1 (CH*Me*$_2$), 27.8 (CH*Me*$_2$), 28.5 (C*H*Me$_2$), 97.7 (γ-C), 126.2, 131.2, 131.8, 150.8 (C ipso), 166.8 (β-C). UV/vis (toluene, 5.0 × 10^{-4} M): 403 nm (ϵ = 1596 L·mol^{-1}·cm^{-1}), 495 nm (ϵ = 1611 L·mol^{-1}·cm^{-1}), 657 nm (ϵ = 993 L·mol^{-1}·cm^{-1}). Green crystals of $[Li(Et_2O)_2][UO_2(Ar_2nacnac)Cl_2]$ (**2**) were grown from the filtered reaction mixture, before the Et_2O was removed in vacuo and the solid was triturated with pentane.

Synthesis of UO$_2$(Ar$_2$nacnac)Cl(Ph$_3$PO) (3). To a solution of complex **1** (0.0287 g, 0.04 mmol) in toluene (2 mL) was added Ph_3PO (0.0121 g, 0.05 mmol), resulting in a color change from green-brown to green-red. This solution was layered with an equal volume of hexanes and stored at −25 °C for 12 h, resulting in the precipitation of green needles. 0.0132 g, 34% yield. Anal. Calcd for $C_{47}H_{56}ClN_2O_3PU$: C, 56.37; H, 5.64; N, 2.80. Found: C, 56.25; H, 5.18; N, 2.54. ^{1}H NMR (C_6D_6, 25 °C, 400 MHz): δ 0.90 (d, 6H, J_{HH} = 6.6 Hz, CH*Me*$_2$), 1.18 (d, 6H, J_{HH} = 6.8 Hz, CH*Me*$_2$), 1.24 (d, 6H, J_{HH} = 6.7 Hz, CH*Me*$_2$), 1.35 (d, 6H, J_{HH} = 6.6 Hz, CH*Me*$_2$), 1.93 (s, 3H, Me), 2.05 (s, 3H, Me), 3.87 (septet, 2H, J_{HH} = 6.7 Hz, C*H*Me$_2$), 3.93 (septet, 2H, J_{HH} = 6.7 Hz, C*H*Me$_2$), 4.95 (s, 1H), 6.93 (m, 6H, meta CH of Ph_3PO), 7.02 (m, 3H, para CH of Ph_3PO), 7.06 (t, 1H, J_{HH} = 7.7 Hz, para CH), 7.17 (d, 2H, J_{HH} = 7.6 Hz, meta CH), 7.25 (t, 1H, J_{HH} = 7.2 Hz, para CH), 7.35 (d, 2H, J_{HH} = 7.6 Hz, meta CH), 7.62 (d of d, 6H, J_{PH} = 12.6 Hz, J_{HH} = 7.4 Hz, ortho CH on Ph_3PO). ^{31}P{^{1}H} NMR (C_6D_6, 25 °C, 162 MHz): δ 65.3.

Synthesis of [UO$_2$(Ar$_2$nacnac)(DPPMO$_2$)][OTf] (4). To a solution of complex **1** (0.0621 g, 0.043 mmol) in toluene (5 mL) was added AgOTf (0.0220 g, 0.086 mmol). The resulting red-brown solution was stirred for 20 min, at which point $DPPMO_2$ (0.038 g, 0.091 mmol) was added to the reaction mixture. This green-brown solution was filtered through a Celite column supported on glass wool (0.5 cm × 2 cm), and the volume of the solution was reduced to 2 mL in vacuo. The filtrate was then stored at −25 °C for 12 h, resulting in the precipitation of brown needles. 0.0693 g, 60% yield. Anal. Calcd for $C_{55}H_{63}UF_3N_2O_7P_2S{\cdot}C_7H_8$: C, 55.36; H 5.32; N 2.08. Found: C, 54.78; H, 5.38; N, 2.20. ^{1}H NMR (C_6D_6, 25 °C, 400 MHz): δ 0.95 (d, 12H, J_{HH} = 6.8 Hz, CH*Me*$_2$), 1.16 (d, 12H, J_{HH} = 6.8 Hz, CH*Me*$_2$), 1.92 (s, 6H, Me), 3.69 (septet, 4H, J_{HH} = 6.4 Hz, C*H*Me$_2$), 4.54 (t, 2H, J_{PH} = 12.8 Hz, CH_2), 4.80 (s, 1H), 6.87 (t, 4H, J_{HH} = 7.6 Hz, para CH on $DPPMO_2$), 6.70 (m, 10H, meta CH on $DPPMO_2$ and para CH), 7.21

(42) Wilkerson, M. P.; Burns, C. J.; Paine, R. T.; Scott, B. L. *Inorg. Chem.* **1999**, *38*, 4156−4158.
(43) Lees, A. M. J.; Platt, A. W. G. *Inorg. Chem.* **2003**, *42*, 4673−4679.

Table 1. X-ray Crystallographic Data for Complexes **1**, **2**, **3**·C_6H_{14}, **4**·2C_7H_8·C_6H_{14}, **5**·$^1/_2C_7H_8$, and **7**·$^1/_2C_7H_8$

	1	**2**	**3**·C_6H_{14}
empirical formula	$C_{58}H_{82}Cl_2N_4O_4U_2$	$C_{37}H_{61}Cl_2LiN_2O_2U$	$C_{53}H_{69}ClN_2O_3PU$
crystal habit, color	plate, green-brown	block, green	needle, green
crystal size (mm^3)	0.13 × 0.13 × 0.04	0.13 × 0.13 × 0.09	0.30 × 0.10 × 0.05
crystal system	monoclinic	monoclinic	monoclinic
space group	$P2_1/n$	$P2_1/n$	$P2_1/c$
volume ($Å^3$)	5954(2)	4132(2)	5103(1)
a (Å)	17.803(3)	17.775(4)	23.370(3)
b (Å)	14.124(2)	12.932(3)	9.610(1)
c (Å)	24.465(4)	19.438(5)	25.184(3)
α (deg)	90	90	90
β (deg)	104.570(3)	112.366(4)	115.539(3)
γ (deg)	90	90	90
Z	4	4	4
formula wt (g/mol)	1446.24	913.75	1086.55
density (calcd) (Mg/m^3)	1.613	1.469	1.414
absorption coefficient (mm^{-1})	5.568	4.094	3.306
F_{000}	2832	1832	2196
total no. reflections	40 348	32 685	39 962
unique reflections	11 818	8505	10 341
final *R* indices [$I > 2\sigma(I)$]	$R_1 = 0.053$, $wR_2 = 0.111$	$R_1 = 0.054$, $wR_2 = 0.125$	$R_1 = 0.083$, $wR_2 = 0.167$
largest diff. peak and hole ($e^-Å^{-3}$)	3.67 and −1.94	3.34 and −0.66	2.68 and −2.15
GOF	0.884	0.921	1.070

	4·2C_7H_8·C_6H_{14}	**5**·$^1/_2C_7H_8$	**7**·$^1/_2C_7H_8$
empirical formula	$C_{75}H_{93}F_3N_2O_7P_2SU$	$C_{59.5}H_{71}F_3N_2O_7P_2SU$	$C_{58.5}H_{71}N_2O_4P_2U$
crystal habit, color	rod, brown	irregular, green-brown	block, orange
crystal size (mm^3)	0.53 × 0.16 × 0.16	0.25 × 0.20 × 0.20	0.20 × 0.20 × 0.08
crystal system	orthorhombic	triclinic	triclinic
space group	*Pbcn*	$P\bar{1}$	$P\bar{1}$
volume ($Å^3$)	14 020(3)	2906.3(8)	2897.8(9)
a (Å)	33.114(5)	13.076(2)	20.737(4)
b (Å)	20.457(3)	13.660(2)	10.882(2)
c (Å)	20.698(3)	17.378(3)	14.340(3)
α (deg)	90	100.768(2)	109.824(3)
β (deg)	90	107.258(2)	106.438(3)
γ (deg)	90	90.241(2)	90.834(3)
Z	8	2	2
formula wt (g/mol)	1523.54	1315.21	1166.14
density (calcd) (Mg/m^3)	1.444	1.503	1.336
absorption coefficient (mm^{-1})	2.453	2.945	2.899
F_{000}	6224	1326	1180
total no. reflections	111 954	23 251	23 687
unique reflections	14 303	11 205	11 457
final *R* indices [$I > 2\sigma(I)$]	$R_1 = 0.058$, $wR_2 = 0.128$	$R_1 = 0.055$, $wR_2 = 0.120$	$R_1 = 0.047$, $wR_2 = 0.112$
largest diff. peak and hole ($e^-Å^{-3}$)	2.12 and −0.79	3.48 and −1.27	4.36 and −0.77
GOF	0.869	0.938	0.929

(d, 4H, J_{HH} = 7.6 Hz, meta CH), 7.88 (m, 8H, ortho CH on $DPPMO_2$). $^{31}P\{^1H\}$ NMR (C_6D_6, 25 °C, 162 MHz): δ 63.2. $^{19}F\{^1H\}$ NMR (C_6D_6, 25 °C, 376 MHz): δ −15.1. $^{13}C\{^1H\}$ NMR (CD_2Cl_2, 25 °C, 125 MHz): δ 24.6 (Me), 26.4 (CH*Me*$_2$), 27.9 (CH*Me*$_2$), 28.7 (C*H*Me$_2$), 125.9, 128.9, 129.6, 129.7 (multiplet, phosphine oxide aryl), 131.9 (multiplet, phosphine oxide aryl), 134.1 (s, phosphine oxide aryl), 136.3, 149.6 (C ipso), 168.3 (*β*-C). UV/vis (CH_2Cl_2, 9.6 × 10^{-4} M): 435 nm (ε = 962 L·mol^{-1}·cm^{-1}), 474 nm (ε = 966 L·mol^{-1}·cm^{-1}), 658 nm (ε = 568 L·mol^{-1}·cm^{-1}). IR (KBr pellet): 1440(s), 1388(s), 1317(m), 1287(s), 1254(s), 1224(m), 1147 (vs), 1093(s), 1031(s), 932(m), 917-(s), 848(w), 793(m), 735(m), 694(m), 637(s), 570(m), 507(m). Complex **4**-d_2 was synthesized in a similar manner. ^2H NMR (C_6H_6, 25 °C, 77 MHz): δ 4.41 (fwhm = 40 Hz).

Synthesis of [UO_2(Ar$_2$nacnac)(Ph$_2$MePO)$_2$][OTf] (5). To a solution of complex **1** (0.0501 g, 0.07 mmol) in toluene (5 mL) was added AgOTf (0.0184 g, 0.07 mmol). The resulting red-brown solution was stirred for 20 min, at which point Ph_2MePO (0.0535 g, 0.24 mmol) was added. This green-brown solution was filtered through Celite supported on glass wool (0.5 cm × 2 cm), and the Celite was subsequently washed with THF until the washings were colorless. The filtrate was layered with hexanes (5 mL) and stored at −25 °C for 12 h, resulting in the precipitation of green oil. Over the course of several days this oil assembled into brown needles. 0.0375 g, 43% yield. Anal. Calcd for $C_{56}H_{67}F_3N_2O_7P_2SU$: C, 53.00; H, 5.32; N, 2.21. Found: C, 53.75; H, 5.37; N, 2.61. ^1H NMR (CD_2Cl_2, 25 °C, 400 MHz): δ 0.82 (d, 12H, J_{HH} = 6.4 Hz, CH*Me*$_2$), 1.16 (d, 12H, J_{HH} = 6.8 Hz, CH*Me*$_2$), 1.35 (d, 6H, J_{PH} = 13.2 Hz, PMe), 1.90 (s, 6H, Me), 3.52 (septet, 4H, J_{HH} = 6.6 Hz, C*H*Me$_2$), 4.80 (s, 1H, *γ*-CH), 7.15 (m, 14H, aryl CH), 7.26, (br s, 8H, ortho CH), 7.53 (t, 4H, J_{HH} = 6.5 Hz, para CH). $^{31}P\{^1H\}$ NMR (CD_2Cl_2, 25 °C, 162 MHz): δ 73.6. $^{19}F\{^1H\}$ NMR (C_6D_6, 25 °C, 376 MHz): δ −13.6. $^{13}C\{^1H\}$ NMR (CD_2Cl_2, 25 °C, 125 MHz): δ 16.1 (d, J_{PC} = 74 Hz, PMe), 24.6 (Me), 25.6 (CH*Me*$_2$), 27.7 (CH*Me*$_2$), 28.3 (C*H*Me$_2$), 100.4 (*γ*-C), 125.6, 128.2, 129.0, 129.6 (d, J_{PC} = 12.5 Hz, phosphine oxide aryl), 131.8 (d, J_{PC} = 10.9 Hz, phosphine oxide aryl), 134.0 (d, J_{PC} = 2.6 Hz, phosphine oxide aryl), 140.1, 148.1 (C ipso), 168.9 (*β*-C). UV/vis (CH_2Cl_2, 6.2 × 10^{-4} M): 406 nm (ε = 871 L·mol^{-1}·cm^{-1}), 485 nm (ε = 936 L·mol^{-1}·cm^{-1}), 671 nm (ε = 491 L·mol^{-1}·cm^{-1}). IR (KBr pellet): 1392(s), 1368(m),

1320(m), 1298(w), 1274(s), 1224(m), 1139(vs), 1091(m), 1067(m), 1032(s), 1000(w), 932(m), 918(s), 890(m), 852(w), 799(m), 780(m), 745(s), 733(w), 718(w), 695(m), 669(w), 637(s), 573(w), 512(s).

Synthesis of UO_2(Ar$_2$nacnac)(CH{Ph_2PO}$_2$) (6). To a solution of complex **1** (0.1039 g, 0.08 mmol) in toluene (2 mL) was added Cp_2Co (0.0161 g, 0.08 mmol). The color quickly changed from green-brown to orange-brown, and a yellow solid precipitated. This solution was stirred for 30 min and was then filtered through a column of Celite supported on glass wool (0.5 cm × 2 cm). The volatiles of the filtrate were removed in vacuo, and the remaining material was rinsed with hexanes (2 mL) to provide a green-brown solid. 0.0334 g, 37% yield. Anal. Calcd for $C_{54}H_{62}UN_2O_4P_2$: C, 58.80; H, 5.67; N, 2.54. Found: C, 58.98; H, 5.78; N, 2.90. ^{1}H NMR (C_6D_6, 25 °C, 400 MHz): δ 1.03 (d, 12H, J_{HH} = 6.6 Hz, CH*Me*$_2$), 1.24 (d, 12H, J_{HH} = 6.8 Hz, CH*Me*$_2$), 2.07 (s, 6H, Me), 2.37 (s, 1H, CH), 3.87 (septet, 4H, J_{HH} = 6.8 Hz, C*H*Me$_2$), 5.02 (s, 1H), 6.99 (m, 12H, meta and para CH on DPPMO$_2$), 7.18 (m, 2H, para CH), 7.28 (d, 4H, J_{HH} = 7.6 Hz, meta CH), 7.62 (m, 8H, ortho CH on DPPMO$_2$). ^{1}H{^{31}P} NMR (C_6D_6, 25 °C, 400 MHz): δ 1.03 (d, 12H, J_{HH} = 6.6 Hz, CH*Me*$_2$), 1.24 (d, 12H, J_{HH} = 6.7 Hz, CH*Me*$_2$), 2.07 (s, 6H, Me), 2.38 (s, 1H, CH), 3.87 (septet, 4H, J_{HH} = 6.5 Hz, C*H*Me$_2$), 5.02 (s, 1H), 6.98 (br s, 4H, para CH on on DPPMO$_2$), 7.00 (br s, 8H, meta CH on DPPMO$_2$), 7.18 (m, 2H, para CH), 7.28 (d, 4H, J_{HH} = 7.6 Hz, meta CH), 7.62 (d, 8H, J_{HH} = 5.2 Hz, ortho CH on DPPMO$_2$). ^{31}P{^{1}H} NMR (C_6D_6, 25 °C, 162 MHz): δ 64.1. ^{13}C-{^{1}H} NMR (C_6D_6, 25 °C, 125 MHz): δ 24.8 (Me), 26.5 (CH*Me*$_2$), 27.5 (CH*Me*$_2$), 28.5 (C*H*Me$_2$), 98.3 (γ-C), 125.2, 128.6, 130.9, 132.4 (m, phosphine oxide aryl), 137.5 (d, J_{HH} = 110 Hz, phosphine oxide ipso), 139.5, 148.4 (C ipso), 167.7 (β-C).

Synthesis of DPPMO$_2$-*d*$_2$. Under an Ar atmosphere Na (0.010 g) was added to D_2O (1.5 mL). After the Na was consumed, DPPMO$_2$ (0.25 g) dissolved in $CDCl_3$ (1.5 mL) was added, and the biphasic mixture was allowed to stir. After 24 h the organic fraction was isolated, dried with $MgSO_4$, and diluted with hexanes (1 mL). This solution was stored at −20 °C for 24 h to provide white crystals. 0.085 g, 34% yield. ^{1}H NMR ($CDCl_3$, 25 °C, 400 MHz): δ 7.34 (m, 8H, meta CH), 7.43 (t of d, 4H, J_{HH} = 7.2 Hz, J_{PH} = 1.6 Hz, para CH), 7.74 (m, 8H, ortho CH). ^{31}P{^{1}H} NMR (C_6D_6, 25 °C, 162 MHz): δ 43.8. ^{2}H NMR (C_6H_6, 25 °C, 77 MHz): δ 3.36 (fwhm = 25 Hz).

Synthesis of UO_2(Ar$_2$nacnac)(Ph$_2$MePO)$_2$ (7). To a green-brown solution of complex **5** (0.0506 g, 0.04 mmol) in toluene (3 mL) was added Cp_2Co (0.0080 g, 0.04 mmol). This resulted in a color change to orange and the formation of a fine yellow precipitate. After 20 min of stirring, the solution was filtered through a Celite column supported on glass wool (0.5 cm × 2 cm). The volatiles were removed in vacuo, and the resulting oil was rinsed with pentane (2 mL) to provide an orange powder. 0.0331 g, 74% yield. Anal. Calcd for $C_{55}H_{67}N_2O_4P_2U$: C, 58.98; H, 6.03; N, 2.50. Found: C, 59.12; H, 5.96; N, 2.53. ^{1}H NMR (C_6D_6, 25 °C, 400 MHz): δ −8.10 (s, 6H, Me), −3.89 (s, 1H, γ-CH), −2.47 (br s, 6H, PMe), −0.31 (s, 12H, CH*Me*$_2$), 1.35 (d, J_{HH} = 6.4 Hz, 4H, meta CH), 3.14 (br s, 2H, para CH), 6.17 (br s, 8H, ortho CH), 6.40 (br s, 4H, para CH), 6.79 (br s, 8H, meta CH), 11.28 (br s, 12H, CH*Me*$_2$), 11.86 (br s, 4H, C*H*Me$_2$). ^{31}P{^{1}H} NMR (C_6D_6, 25 °C, 162 MHz): δ −28.7 (fwhm = 80 Hz). UV/vis (toluene, 2.92 × 10^{-3} M): 471 nm (ϵ = 688 L·mol^{-1}·cm^{-1}), 615 nm (ϵ = 74 L·mol^{-1}·cm^{-1}), 717 (shoulder, ϵ = 27 L·mol^{-1}·cm^{-1}), 755 (ϵ = 56 L·mol^{-1}·cm^{-1}). IR (KBr pellet): 1368(m), 1320(s), 1264(w), 1228-(w), 1168(s), 1147(m), 1125(m), 1100(m), 1072(w), 1028(w), 998(w), 929(w), 922(w), 891(s), 840(w), 808(s), 800(s), 776(m), 745(s), 715-(m), 695(s), 512(m).

X-ray Crystallography. The crystal structures of complexes **1**, **2**, **3**·C_6H_{14}, **4**·2C_7H_8·C_6H_{14}, **5**·$^1/_2C_7H_8$, and **7**·$^1/_2C_7H_8$ were determined similarly with exceptions noted in the Supporting Information. Crystals were mounted on a glass fiber under Paratone-N oil. Data collection was carried out a Bruker 3-axis platform diffractometer with SMART-1000 CCD detector. The instrument was equipped with graphite monochromatized Mo Kα X-ray source (λ = 0.710 73 Å). All data were collected at 150(2) K using Oxford nitrogen gas cryostream system. A hemisphere of data was collected using ω scans, using 10- to 20-s frame exposures and 0.3° frame widths. SMART[44] was used to determine the cell parameters and data collection. The raw frame data were processed using SAINT.[45] The empirical absorption correction was applied based on Psi-scan. Subsequent calculations were carried out using SHELXTL.[46] The structures were solved using Direct methods and difference Fourier techniques. All hydrogen atom positions were idealized and rode on the atom of attachment. The final refinement included anisotropic temperature factors on all non-hydrogen atoms. Structure solution, refinement, graphics, and creation of publication materials were performed using SHELXTL or WinGX.[47]

Solvent molecules of hexane and/or toluene were found to cocrystallize into the crystals of **3**, **4**, **5**, and **7**, and most of the solvent molecules had large thermal displacements or positional disorder. The atoms of the disorder solvent molecules were refined isotropically, while the C−C distances were fixed at 1.52 Å. The hydrogens attached to the disordered atoms were not added. X-ray crystallographic data for **1**, **2**, **3**·C_6H_{14}, **4**·2C_7H_8·C_6H_{14}, **5**·$^1/_2C_7H_8$, and **7**·$^1/_2C_7H_8$ can be found in Table 1.

Acknowledgment. We thank the University of California, Santa Barbara for financial support of this work. We also thank Dr. Alexandre Mikhailovsky for assistance with the UV/vis and fluorescence measurements.

Supporting Information Available: X-ray crystallographic details (as CIF files) of **1**, **2**, **3**·C_6H_{14}, **4**·2C_7H_8·C_6H_{14}, **5**·$^1/_2C_7H_8$, and **7**·$^1/_2C_7H_8$; tabulated cyclic voltammetry data for **4** and **5**; fluorescence spectrum of **4**; IR spectra of **5** and **7**; ^{1}H NMR spectra of **7** in C_6D_6, THF-d_8, and C_6D_6/CD_2Cl_2. This material is available free of charge via the Internet at http://pubs.acs.org.

JA077538Q

(44) *SMART Software Users Guide*, version 5.1; Bruker Analytical X-ray Systems, Inc.: Madison, WI, 1999.
(45) *SAINT Software Users Guide*, version 5.1; Bruker Analytical X-ray Systems, Inc.: Madison, WI, 1999.
(46) Sheldrick, G. M. *SHELXTL*, Bruker Analytical X-ray Systems, Inc.: Madison, WI, 2001.
(47) Farrugia, L. J. *J. Appl. Crystallogr.* **1999**, *32*, 837−838.